What Embedded LDV measurements can do for boundary layer investigation of rotating blades.

by
C. Barla, E. Berton, D. Favier, C. Maresca, M. Nsi Mba

Laboratoire d'Aérodynamique et de Biomécanique du Mouvement,
CNRS & Université de la Méditerranée
163 Av de Luminy, 13288 Marseille cedex 09, France
Tel :33 4 91 266030 ; Fax :33 4 91 411691
eric@morille.univ-mrs.fr

Abstract

The present paper concerns the original work undertaken at LABM to determine the boundary layer velocity distribution in the inboard region of a tilt-rotor blade by using an Embedded Laser Doppler Velocimetry method (ELDV).

The experiments were carried out on a two bladed tilt-rotor with complex blade geometry. A blade section close to the hub was explored in three chord stations, for 2 pitch angles, one at a value lower than the static stall angle and the other one at a higher value. Results obtained on the velocity components allow characterizing the different features of the boundary layer (BL). In particular, a delay of the BL separation due to the blade rotation has been observed at high incidence. Such a delay is revealed by experimental velocity profiles measured inside the boundary layer region. In particular, the spanwise component has been useful to specify the centripetal or centrifugal character of the flow over the blade section. The present results have shown that the ELDV method is quite able to measure velocity profiles in the BL of a rotating blade and to qualify its nature with the validation of the transitional criteria based on the calculation of the second thickness of energy δ'_3.

Notations

a	Speed of sound, m/s
C	Airfoil chord, m
f	Rotational frequency, Hz
n	Rotational frequency, rpm
M_{tip}	Tip blade Mach number: $M_{tip}=\Omega R/a$
R	Rotor radius, m
Re	Reynolds number, $Re_r=\Omega rc/\nu$
U_e	External velocity at section r/R=0.3
V_t	Tangential velocity, m/s
V_r	Crossflow velocity, m/s, "+" centripetal, "-" centrifugal
z	Normal distance to the surface of the blade section, m
α	Angle of attack of the blade section, deg
δ'_3	Second thickness of energy of the boundary layer, m

$$\delta_3' = \int_0^{\delta} \frac{Vt^2}{Ue^2} * (1 - \frac{Vt}{Ue}) dz$$

η	Reduced normal distance to the surface $\eta=z(U_e/\nu x)^{1/2}$
θ	Collective pitch angle of the blade section, deg
Ω	Rotational frequency, rad/s

Introduction

The accurate prediction of unsteady aerodynamics associated with rotating blade performances is of major interest in a wide range of aeronautical applications. For example, the dynamic stall occurring on the retreating blade of an helicopter rotor in forward flight produces significant changes in the airloads and moments spanwise distributions, and thus in the overall rotor performance (Ref.1 to 6). A better understanding of the unsteady Boundary-Layer (BL) evolution leading to dynamic stall undergoes a proper simulation of the complex blade sections environment and requires considering the influence of several parameters, including simultaneous variations in both angle-of-attack and local flow velocity, compressibility effects, blade tip effects, airfoil geometry and sweep angle influence, as well as crossflow and separation phenomena influences.

However, due to the complex nature of the 3D unsteady stall phenomenon, previous works in this domain have generally tackled the problem by means of simplified flow configurations, which are simulated to specifically dissociate the different parameters in order to analyze separately their respective influence.

LABM has developed for many years researches focused on dynamic stall on oscillating airfoils (mainly in fore-and-aft,

pitching and translation/pitch combined motions (Ref. 7 to 9), and on local flow field around helicopter rotor blades in hover and forward flights. These studies have allowed the improvement of original embedded Laser Doppler Velocimetry (ELDV) methods for detailed and accurate measurements of the flow very close to moving walls (boundary-layers) and in their near wakes (Ref 10 to 12).

This paper concerns the original work undertaken at LABM to determine the boundary layer velocity distribution in the inboard region of a tiltrotor blade by using an Embedded Laser Doppler Velocimeter located in a blade section close to the hub. The purpose of the present research is to extend experiments based on the ELDV method applied on a simple rotating blade to a more sophisticated blade with non linear twist, thickness and airfoil spanwise distributions as close as possible to a blade tilt-rotor characteristics (Ref. 13).

The paper successively presents the tiltrotor blade geometry and the hovering flight parametric conditions relative to our study. A detailed description of the LDV Velocimeter characteristics and its embedment is given before showing how the velocity components (chordwise V_t and spanwise V_r) are deduced from the ELDV measurements. The velocity results obtained for 2 pitch angles (one below the static stall angle e.g. θ=15.38deg and one above the static stall angle e.g. θ=24.75deg) are then analyzed and with respect to the behavior of the boundary layer, in particular at high pitch angle where stall delay due to rotational effect has been observed.

Experimental set-up and Measurements methods

The rotor blade geometry is similar to the one of CAMRAD II model of TRAM (Ref.14). The linear part of the twist, relative to the blade sections located in the region close to the rotor hub, allows to easily implement an optical head and a 45deg mirror in a spanwise r/R section where converging laser beams emerge to create the measurement volume. For three chordwise stations x/c=0.10, 0.33 and 0.54 located at r/R=0.3, the tangential and crossflow velocity components have been measured in the boundary layer from 0.3 to 20mm along the normal distance to the wall (corresponding to $1<\eta<80$).

Rotor Blade Geometry and the model scale of rotor. The geometry of the blade is similar to those of CAMRAD II of TRAM. In order to have the same solidity σ=0.1 for a 2-bladed rotor, the following geometry of the blade has been adopted:

Rotor Radius: R=1.5m
Blade Length: l=1.26m
Solidity: σ=0.1
Number of Blades: 2

Twist and chord distributions of the blade are respectively given in Fig.1. The twist law distribution is given with the conventional twist=0 for r/R=0.75. Three different airfoils of NACA series have been distributed all along the span (NACA 64528, 64118 and 64152) as sketched in Fig.2.
As shown in Fig.3, the model scale of rotor is set up on the hovering test rig of LABM. The rotor is operating in hover with an induced flow blowing from the bottom to the top in order to minimize ground and recirculation effects.

Experimental Apparatus : the Embedded LDV. The main components of the Laser Doppler Velocimeter are embedded in the rotating blade by use of a prototype probe (see Fig.4) of 0.22m length in the span direction. As shown in Fig.2, the probe can be set at different positions in order to explore 3 chordwise stations.

Two parallel beams coming from the optical fibres arrive through the probe to the lens, converge to the mirror and focalize through the optical window in the measurement volume (see Fig.4). The measurement volume can be displaced normally to the optical window by means of a translation screw, which changes the relative position between the lens and the mirror. The more the lens is far from the mirror, the more the measurement volume is close to the blade surface. The laser beams issued from the laser source are conduced to the blade through fixed optical fibres, a light transmitter and rotating optical fibres connected to the rotating blade by the guiding tube. (see Fig.5). The rotating transmitter is the most critical part of the ELDV method. First it transmits the input laser beam on axis during rotation while maintaining a constant linear polarization. Secondly, it transmits the received light in a coaxial mode to an external multimode fiber link. The signal light coming back from the probe is guided out to a fixed photo detector and signal processor.
The picture in Fig.6 shows the laser beams focused in the measurement volume very close to the blade surface. The seeding of the

flow is realized by emitting particles of oil mixture (about 1µm in diameter) in the entire hovering hall where the rotor is running.

Table 1 gives the main characteristics of the ELDV system with the dimensions of the measurement volume. The dz length allows a measurement at the wall as close as 0.3mm and the focal lens provides an exploration along the normal to the wall of 20 mm.

Table 1. Laser velocimeter specifications

	Specification	Units
Velocity component	1D*: tangential Vt or spanwise Vr	m/s
Focal lens	50	mm
Laser source wave length	514,5	nm
Measurement volume	dx=0.041 dz=0.510	mm mm
Fringe spacing	0.0032	mm
number of fringes	13	
Axial working length	46	mm

Measurement of velocity components V_t and V_r. As shown in Fig. 7, the measured velocities U42 and U37 allow the reconstruction of the tangential V_t and radial V_r velocity components. At each x/c chord position, the probe can be positioned in 2 different fixed positions obtained by rotating the probe around its axis. By construction, in the first position the angle between the measured velocity U42 and the chord direction is 42deg while in the second position the angle between the measured velocity and the chord direction is 37deg (see Fig.7).

According to Fig.7, the radial and chordwise velocity components are given by :

Equations(1)

$$V_t = U42*\cos(42deg) - U37\cos(37deg)$$

$$V_r = -U42*\sin(42deg) - U37\sin(37deg)$$

Data acquisition. Backscattered signals from the measurement volume are analyzed through BSA during a running time comprised between 3 seconds and 3minutes, depending on the BL region explored. This time is used to acquire 4000 samples of the U42 or U37 velocity components. The data are recorded as presented in Fig.8 over a single period, and statistically reduced (rms value, histogram, mean value,…). Fig.9 presents an example of the histogram relative to the U42 velocity component.

Fig.10 presents an example of the variation with z of the U42 and U37 velocity components obtained as described above. Components V_t and V_r are then obtained from equations (1).

Experimental uncertainty: the uncertainty of the ELDV used in a rotating blade has been evaluated in detail (Ref.15). It has been shown that the maximum measurement error on V_t is less than 2.6% and less than 6% concerning the V_r component.

Results and Discussion

First experiments have been conducted at a relatively low rotation speed (480rpm) in order to adjust the embedded velocimeter method. Table 2 presents the parametric conditions relative to these measurements :

Table 2: Test conditions and data acquired : r/R=0.3; n=580rpm; M_{tip}=0.22

Pitch angle $\theta_{r/R=0.3}$	15.38deg	24.75deg
Chord station x/C	0.1; 0.33; 0.54	0.1; 0.33; 0.54
Data acquired	V_t; V_r	V_t; V_r
Z explored in mm	0.3-19	0.3-19

The results analysis and particularly the aerodynamic behavior around the airfoil section enlightened by the BL velocity profiles require the knowledge of the local angle of attack of the airfoil section which is deduced from the θ collective pitch angle and the α_i induced incidence. α_i has been obtained from the direct measurement of the induced velocity field. For θ=15.38deg, the local angle of attack value is equal to α=13.2deg, while for high collective pitch angle θ=24.75deg, the local angle of attack correspond to α=19.1deg.

Experimental results on V_t and V_r have been gathered in Fig.11 and 12. The (V_t, V_r) couple versus the distance to the wall z is presented at the two pitch angle values α, and for the

three chord stations x/c (respectively noted A,B,C).

It can be seen from results in Fig.11 that the chordwise component V_t increases with the incidence in the potential flow at each chord station (see A, B, C). This result, expected in the case of an unstall airfoil, becomes unexpected at θ=24.75deg, where the angle of attack has been estimated at 19.1deg, corresponding to an incidence where the BL should be separated. When examining the velocity profile in the BL at x/c=0.33 (Fig.11B), it can be concluded that the BL at θ=24.75deg is attached and the shape of the profile correspond to a turbulent evolution. At x/c=0.54 (see Fig.11C), the velocity profile measured at α=24.75deg in the BL has thickened in the z direction which reveal a separation tendency. Moreover, in order to determine the nature of the BL, comparisons are provided in Fig.13 to 16 for each chord station, the measured velocities with different theoretical velocity evolutions corresponding to :
- the exact solution of Blasius (laminar velocity profile without pressure gradient),
- a 4th polynomial order of Pohlhausen (laminar velocity profile with pressure gradient),
- a turbulent profile with a 1/n law evolution.

Fig.14B also shows, for x/c=0.10 that the Pohlhausen parameter Λ has to reach a very high value (more than 20) in order to fit experimental velocity profiles. Such a value is synonymous of a very high pressure gradients as regard to airfoils oscillating in pitch, where $-12 < \Lambda < 12$. In the present case, centrifugal effects appear to increase the pressure gradient at the leading edge while reducing the BL thickness (Fig.14B). For x/c=0.33 and 0.54 and θ=24.75deg (Fig. 15B and 16B), the experimental velocity profiles present a turbulent evolution and are very well fitted by a 1/n theoretical velocity profile.
Even for a high value of collective pitch (θ=24.75deg), it appears that the BL remains reattached.

When considering the velocity evolution at x/c=0.10 and x/c=0.33 at θ=15.38deg, it clearly appears that the BL present a laminar evolution. The theoretical velocity profiles obtained respectively from the Blasius solution or from the Pohlhausen polynomial well fit the experimental velocity profiles at x/c=0.10 (Fig.13A, Fig.14A) and x/c=0.33 (Fig.15A). For x/c=0.54 and θ=15.38deg, Fig.16A shows that a turbulent profile with 1/n law evolution has to be chosen to characterize the experimental V_t evolution.

In order to confirm the nature of the BL, a transitional criterion previously establish at LABM (Ref.8-11) and based on the calculation of the second thickness of energy δ'_3 have been applied for the two collective pitch angles. The following equation gives the formulation of this criterion which is able to detect the transition of the BL from a laminar state to a turbulent one:

$$(Re_{\delta'3})_t = 0.0135*(1+1.5e^{-(Rex/35000)})*Re_x^{0.8}$$

Fig.17 illustrates the application of such a criterion for the two collective pitch angles θ=15.38deg and θ=24.75deg. For Fig.17A (θ=15.38deg), it is shown that the BL layer presents a laminar evolution at x/c=0.10 and 0.33, while a turbulent evolution appears for x/c=0.54. Fig.17A allows to determine the transition point of the BL which is located in chord after x/c=0.33 (approximately around x/c=0.35). For θ=24.75deg (Fig.17B) the BL is laminar only for x/c=0.10 and the transitional point appears to be located near the leading edge (x/c=0.18).
These results confirm the evolution of experimental and theoretical velocity given in Fig.13 to 16.

It can also be concluded that the dynamic stall phenomenon has not been observed during this experiments which indicate an important delay of the BL separation due to rotation (in terms of collective pitch values).

The crossflow component remains difficult to analyze inside the BL because of the uncertainty of measurements that increases very close to the wall. Nevertheless, a better precision on V_r in the potential flow allows obtaining information on the direction of the flow at different chordwise station of the airfoil section. The following table 3 gives the centrifugal or centripetal tendency of the flow over the blade section, with on the right part the flow directions at different θ, sketched by black arrows. This table has been elaborated from the results obtained from Fig. 11A, 11B, 11C and 12B.

Table 3 Evolution of the crossflow velocity as a function of θ and x/C

x/c \ θ	15.38	24.75
0.10	Centrifugal -1m/s	Centripetal 2m/s
0.33	Centripetal 1m/s	Centrifugal -1m/s
0.54	Centripetal 3.5m/s	Centrifugal -1m/s

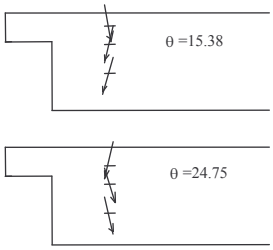

Conclusions

The boundary layer over the upper side surface of a tilt rotor blade has been explored in the inboard region near the hub by means of an Embedded Laser Doppler Velocimeter method (ELDV). Chordwise and spanwise components have been measured at the blade section r/R=0.3, for a constant tip Mach number M_{tip}=0.22, three chord stations x/C=0.10; 0.33; 0.54 and two collective pitch angles θ=15.38 and 24.75deg.

The analysis of the velocity components measured along the normal to the airfoil section in the BL and part of the potential flow, from 0.3mm to 20mm (1≤ η ≤80), has pointed out the following conclusions:

-At θ=15.38deg and x/C=0.54, chordwise velocity profiles exhibit a BL turbulent behavior (1/n law). For x/C=0.10 and 0.33, the BL appears to be very thin with a laminar velocity profile.
-At θ=24.75deg, it is worthy to note that the chordwise velocity profile relative to x/C=0.33 shows an attached turbulent BL. This particular result indicates a delay of the BL separation due to rotation.
-The spanwise velocity component is very useful to specify if the flow passing over the blade section is centripetal or centrifugal, but the characterization of the BL behavior in the radial direction remains difficult to identify from the V_r evolution.

This work has also contributed to extend the validation of a transition criterion (previously establish at LABM) which is based on the calculation of the second thickness of energy δ'_3. In future work, this transition criterion has to be validated for other parametric conditions (collective pitch angles, rotational frequencies, x/c positions …).

The present results have shown that the ELDV is well adapted to measure velocity profiles inside the BL of a rotating blade and to qualify its nature. This work will constitute a useful database for future computational unsteady boundary layer and CFD methods applied to tiltrotor blade aerodynamics.

Acknowledgements

This research is partly supported by the USARDSG-UK under contract N62558-02-M5609. The authors are particularly thankful to Dr. Chee Tung for his fruitful advices and encouragements during the work.

References

1- C. MARESCA, D. FAVIER, J. REBONT, “Experiments of an Aerofoil at High Angle of Incidence in Longitudinal Oscillations”, Journal of Fluid Mechanics, Vol. 92, Part 4, 1979.

2- W.J. Mc CROSKEY, “The Phenomenom of Dynamic Stall”, NASA TM 81264, March 1981.

3- L.E. ERICSON, J.P. READING, “Unsteady Flow Concepts for Dynamic Stall Analysis”, Journal of Aircraft, Vol. 21, N° 8, pp. 601-606, August 1984.

4- T.S. REDDY, K.R. KAZA, “A Comparative Study of Some Dynamic Stall Models”, NASA TM 88917, March 1987.

5- D. FAVIER, A. AGNES, C. BARBI, C. MARESCA, "Combined translation/pitch motion : a new airfoil dynamic stall simulation.", Journal of Aircraft, Vol. 25, N° 9, pp. 805-814, 1988.

6- J.G. LEISHMAN, T.S. BEDDOES, “A Semi-Empirical Model for Dynamic Stall”, Journal of American Helicopter Society, Vol. 34, pp. 3-17, July 1989.

7- W. J. Mc CROSKEY, K.W. Mc ALISTER, L.W. CARR, and S.L. PUCCI, “An Experimental Study of Dynamic Stall on advanced Airfoils sections Volume 1. Summary of Experiments”, NASA TM 84245, July 1982.

8- E. BERTON, D. FAVIER, C. MARESCA, “Embedded L.V. methodology for boundary-layer measurements on oscillating models”, A.I.A.A., Proceedings of the 28th Fluid Dynamics Conf., A.I.A.A. paper n° 97/1832, Snowmass, June 1997.

9- E. BERTON, D. FAVIER, C. MARESCA, “Experimental and numerical investigation of dynamic stall at IRPHE/ASI Laboratory”, 24th European Rotorcraft Forum, Cheeseman Award Presentation, Marseille 1998.

10- D. FAVIER, C. MARESCA, M. NSI MBA, E. BERTON, A. AGNES, “New Type of Embedded Laser Doppler Velocimeter (ELDV) for Measurement of Rotary Wings Boundary-Layer”, The Review of Scientific Instruments, Vol. 66, n° 6, pp. 2447-2455, 1997.

11- E. BERTON, D. FAVIER, C. MARESCA, M. NSI MBA, “Application of Laser Doppler Velocimetry to unsteady flow around rotating blades” Proc of 10th International Symposium on Applications of Laser Techniques to Fluid Mechanics, Lisbon, 10-14 July 2000.

12- C. MARESCA, E. BERTON, D. FAVIER, A. BENYAHIA, “Study of 2D and 3D boundary layer of moving walls by embedded LDV measurements” Final Technical Report N° 68171-01-M-5090, ERO of the US Army, March 2002.

13. C. MARESCA, E. BERTON, D. FAVIER, “Embedded LDV Measurements in the Boundary Layer of Moving Walls”, Final Technical report, ERO Contract n° N 68171-99-M-6670, December 2000.

14- JOHNSON W., “Airloads and wake geometry calculations for an isolated tiltrotor model in a wind tunnel”, Proceedings of the 27th European Rotorcraft Forum, Moscow, Russia, September 11-14, 2001.

15- DEPARIS M., “Application d’une technique de mesure basée sur la Vélocimétrie Laser Embarquée à l’étude de la couche limite développée sur une pale de rotor d’hélicoptère”, Thèse de Doctorat de l’Université Aix-Marseille II, 30 septembre 1998.

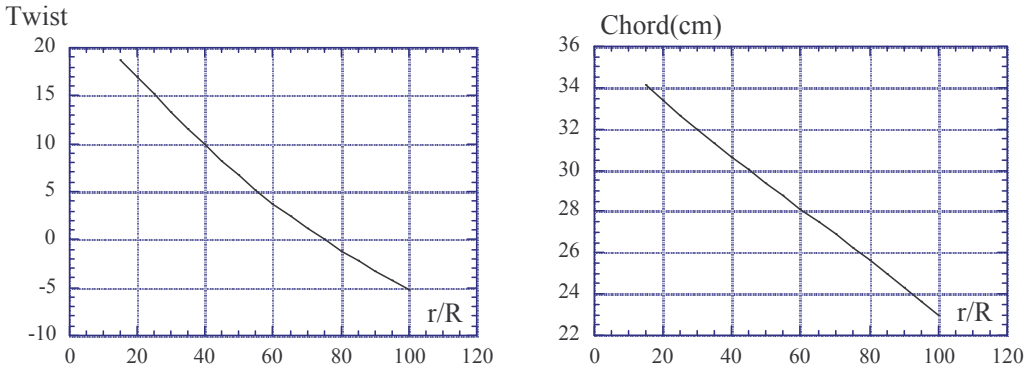

Fig.1: Twist and Chord distributions along the blade span

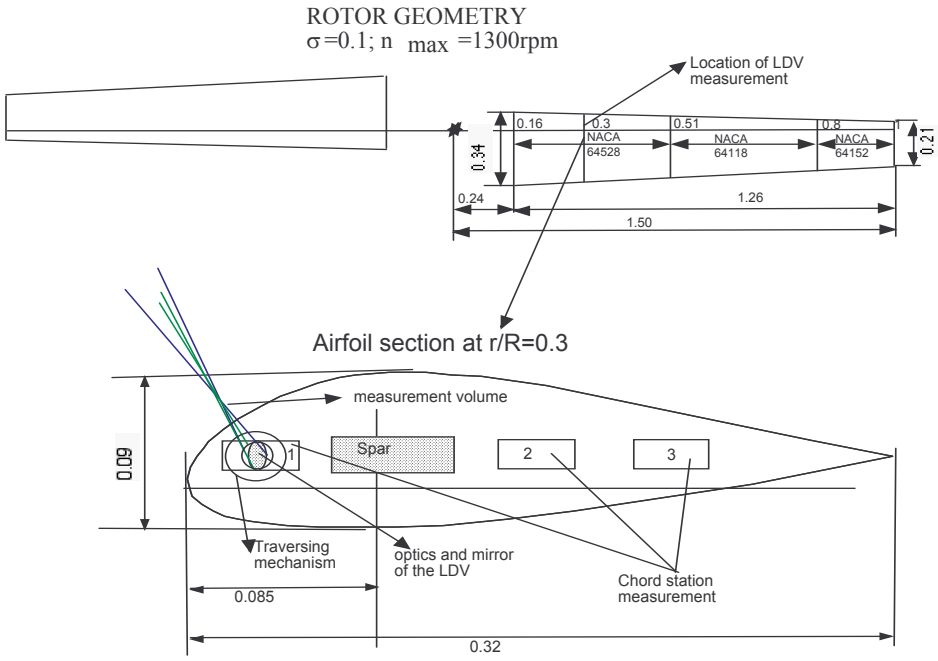

Fig.2: Rotor geometry and airfoil section characteristics

Fig.3: View of the rotor in the hall of S1L

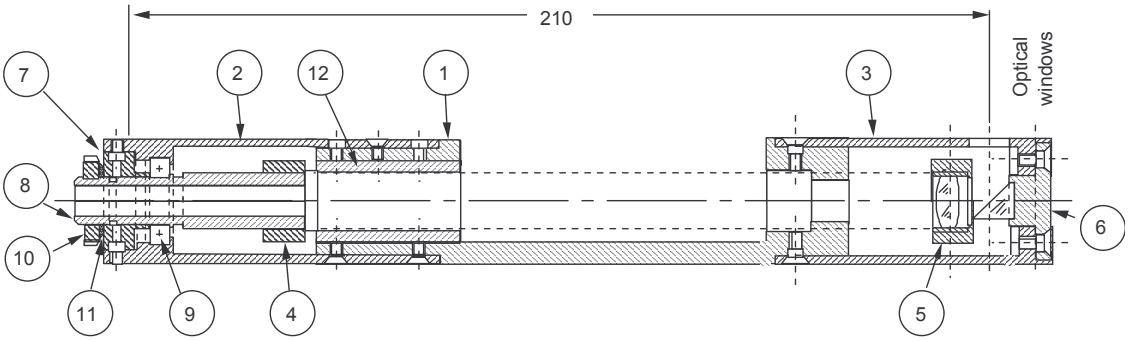

Rep	Description
12	Laser probe block piece
11	MB1 brake ring
10	SKF KM1 nut
9	Rigid bearing
8	Translation screw
7	Bearing block piece
6	Mirror support
5	Lens support
4	Lens displacement piece
3	Cownstream cover
2	Upstream cover
1	Laser probe support

Laser probe set-up

Fig.4: Embedded laser probe set-up

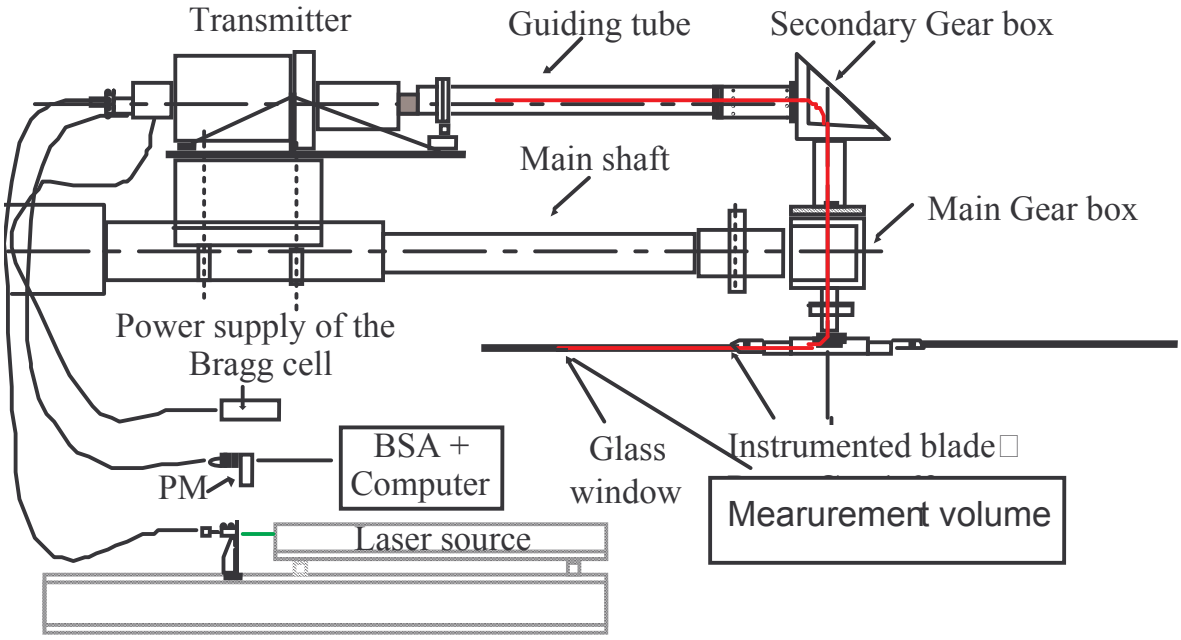

Fig.5 : Schematics of the Embedded Laser Doppler Velocimetry method.

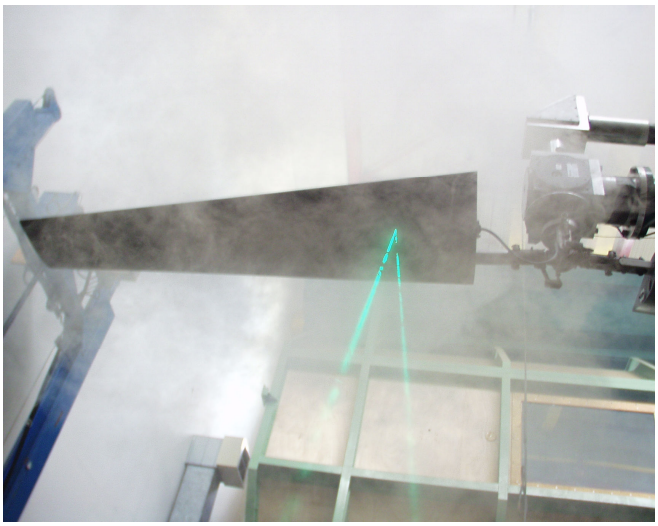

Fig.6 : View of the blade and measurement volume

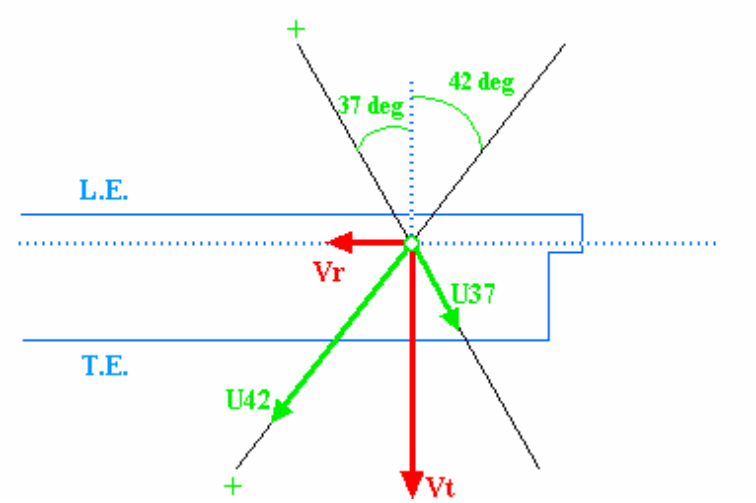

Fig.7 : Principle of velocity measurements V_t and V_r

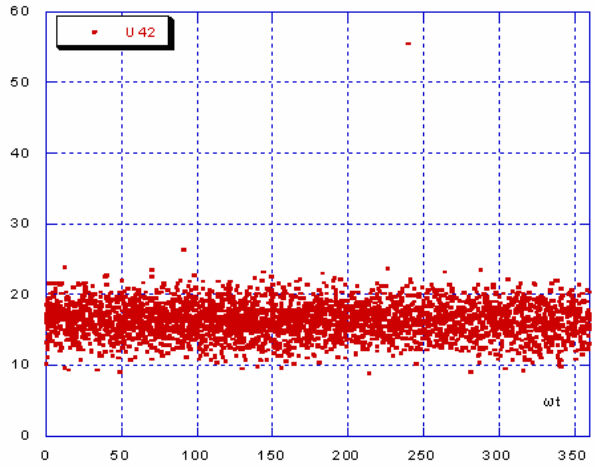

Fig.8 : Example of U42 data acquisition presented over a single period (4000 data). θ=15.38deg and x/c=0.54

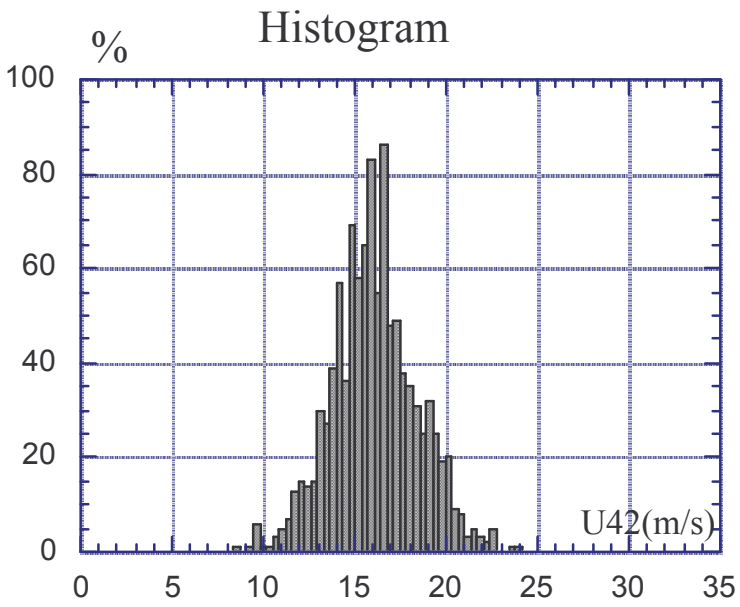

Fig.9: Example of histogram obtained on the U42 component.

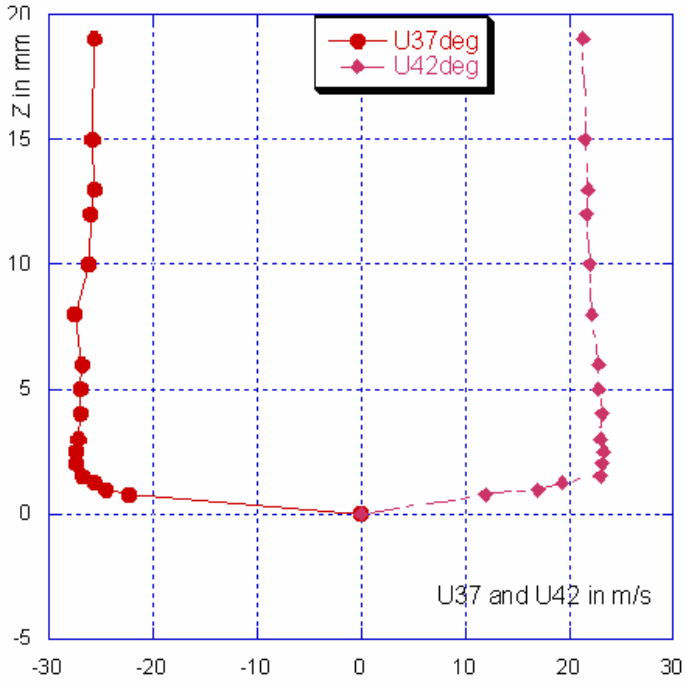

Fig.10: Evolution of the velocity component measured at α=15.38 deg and x/c=0.33

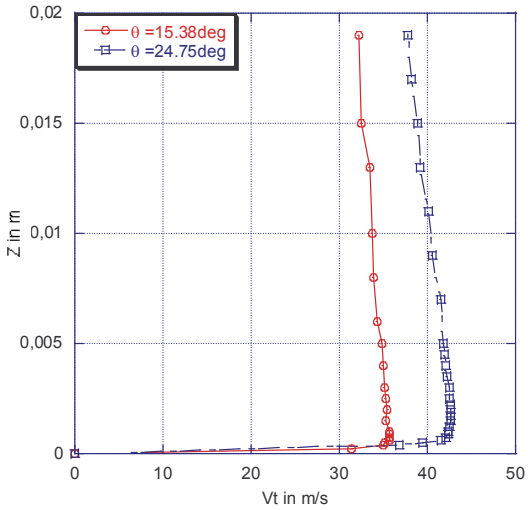

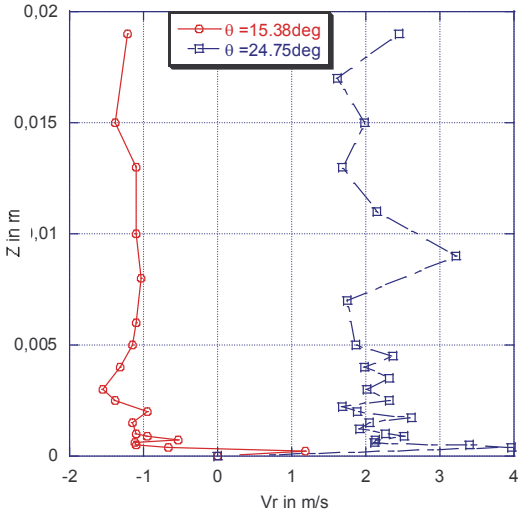

A
x/c=0.10

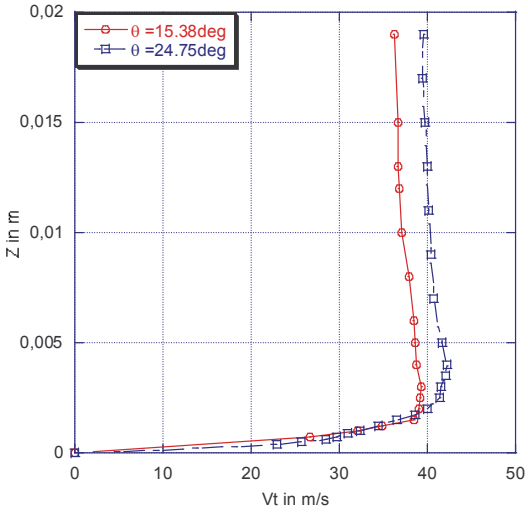

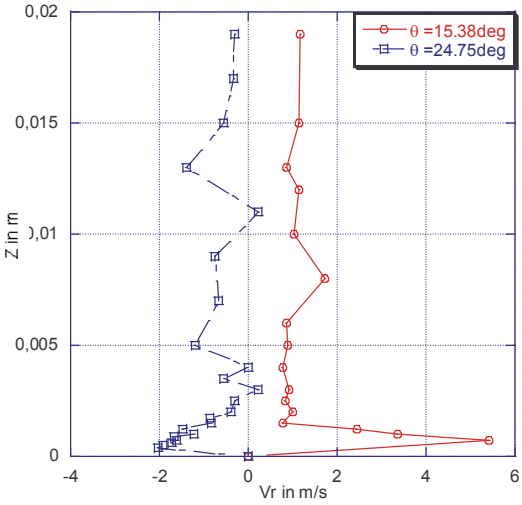

B
x/c=0.33

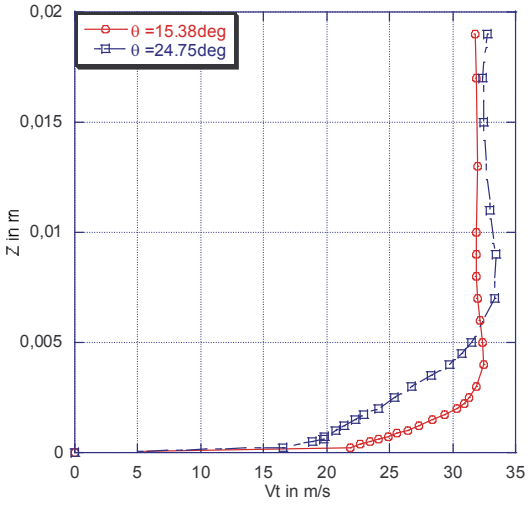

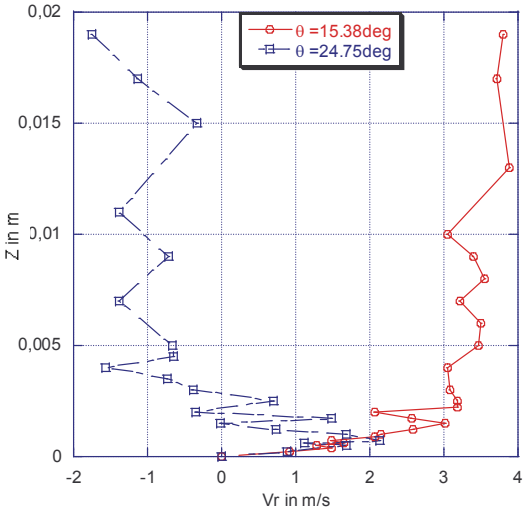

C
x/c=0.54

Fig.11 : Evolution of Vt and Vr as a function of z for 2 θ values at x/c=0.1, 0.33, 0.54

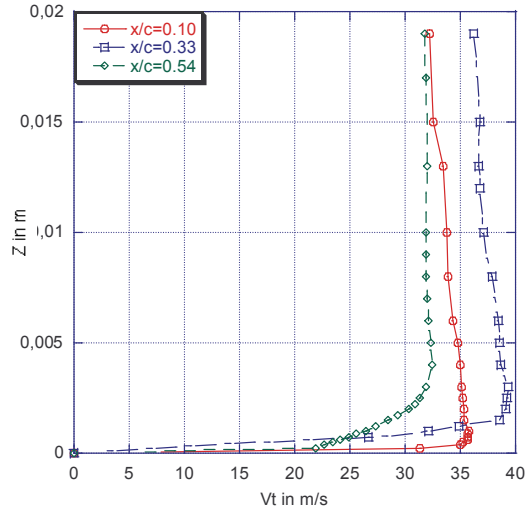

θ=15.38deg

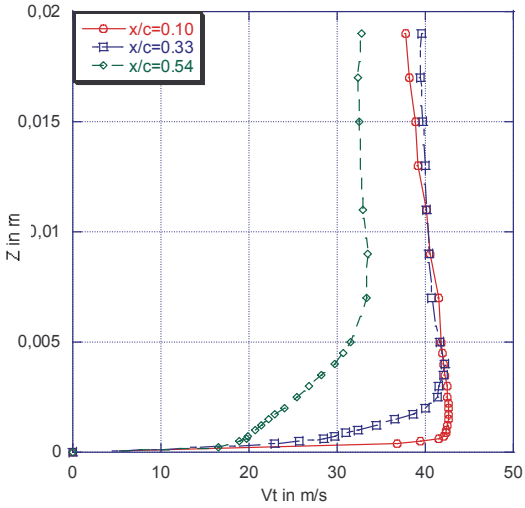

θ=24.75deg

A

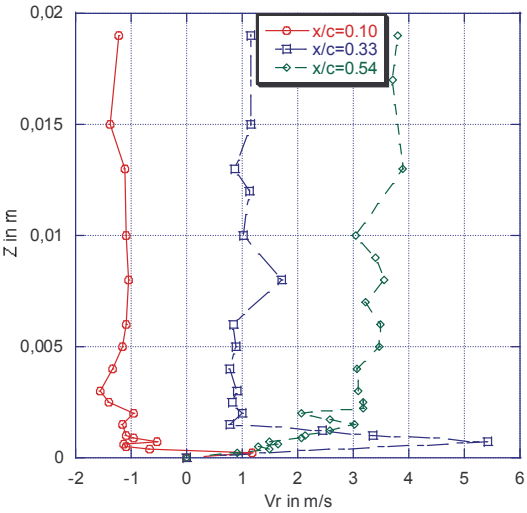

θ=15.38deg

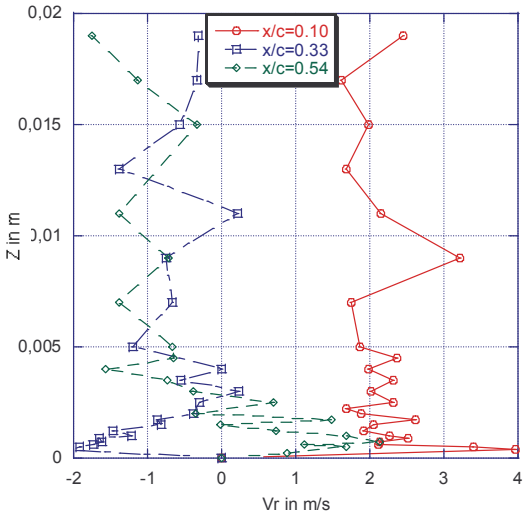

θ=24.75deg

B

Fig. 12 : Evolution of V_t (A) and V_r (B) as a function of z for different x/c values at θ=15.38 and 24.75deg

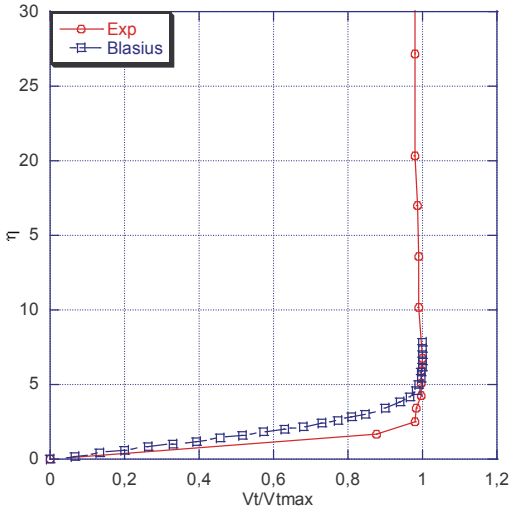

A : θ=15.38deg

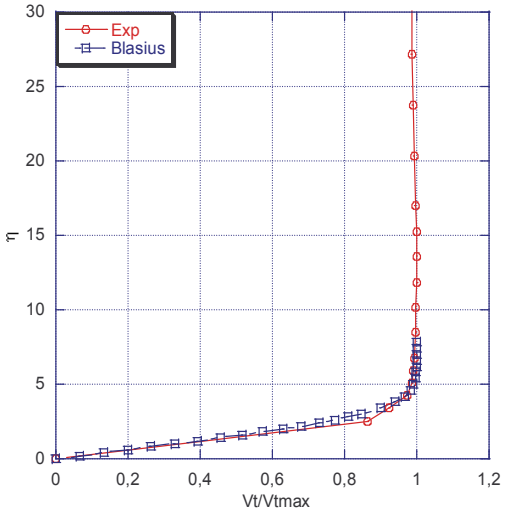

B : θ=24.75deg

Fig.13 : Comparison of V_t/V_{tmax} with the exact solution of Blasius for x/c=0.10

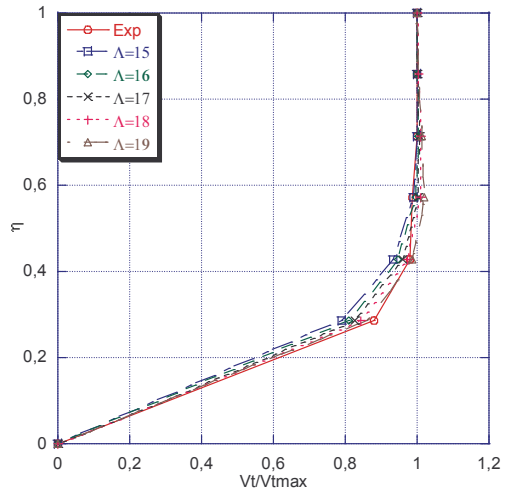

A : θ=15.38deg

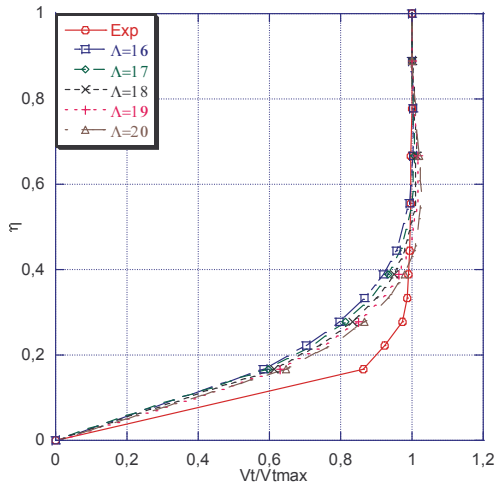

B : θ=24.75deg

Fig.14 : Comparison of V_t/V_{tmax} with the 4th polynomial order of Pohlhausen for x/c=0.10

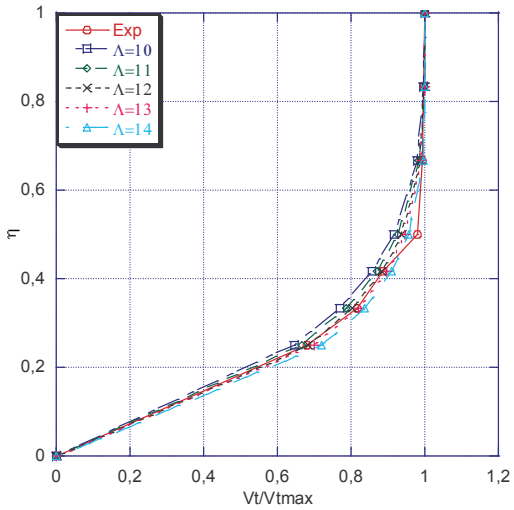

A : θ=15.38deg

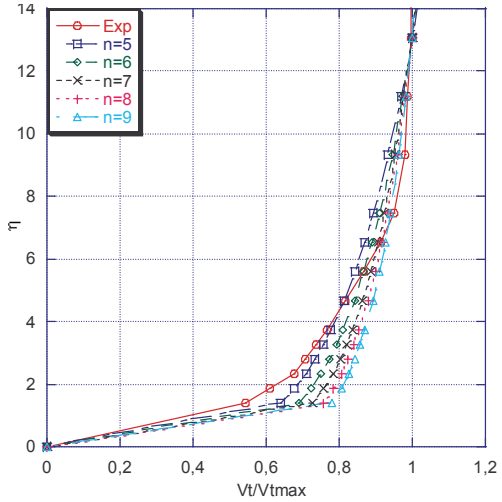

B : θ=24.75deg

Fig.15 : Comparison of V_t/V_{tmax} with Pohlhausen (A) and 1/n law (B) velocity profiles for x/c=0.33

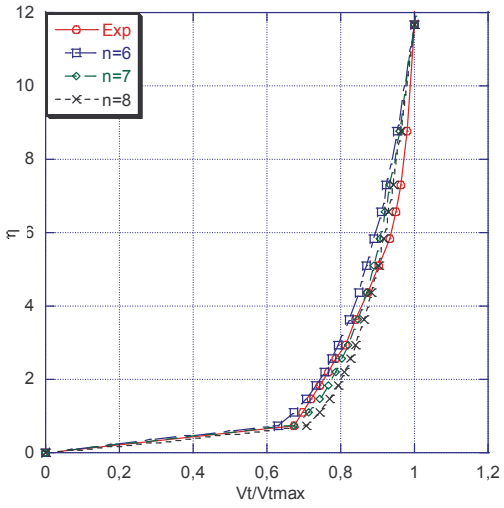

A : θ=15.38deg

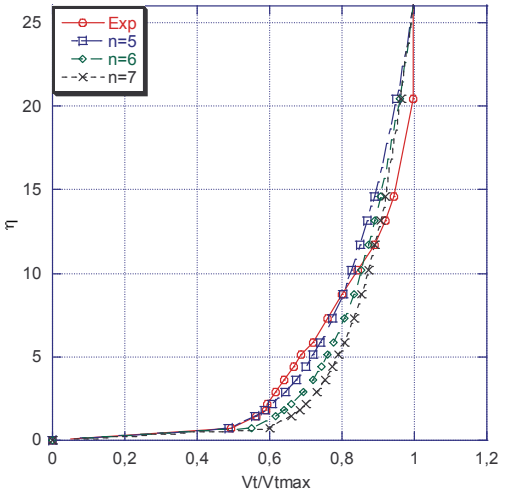

B : θ=24.75deg

Fig.16 : Comparison of V_t/V_{tmax} with 1/n law velocity profiles for x/c=0.54

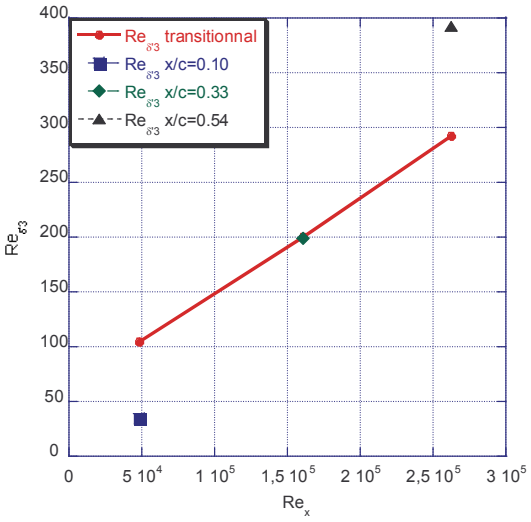

A : θ=15.38deg

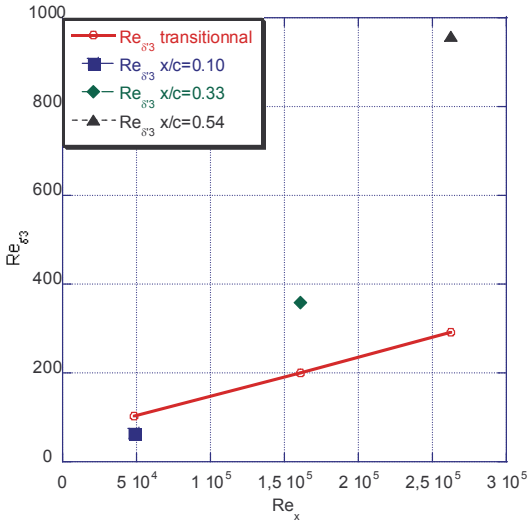

B : θ=24.75deg

Fig.17 : Transitional criterion $Re_{\delta'3}=f(Re_x)$